



## Article Info

Received: 22<sup>nd</sup> September 2024Revised: 14<sup>th</sup> October 2024Accepted: 19<sup>th</sup> October 2024

Department of Physics, University of  
Port Harcourt, P.M.B 5323, Choba, Port  
Harcourt, Rivers State, Nigeria

\*Corresponding author's email:

[analemnkem@gmail.com](mailto:analemnkem@gmail.com)Cite this: *CaJoST*, 2024, 3, 360-370

## 1. Introduction

Diffusion is a fundamental process in material science, characterized by the movement of atoms and molecules from one site to another in a material medium due to thermal agitation. This results in a uniform composition throughout the material. As defined by Rajput [1], diffusion is driven by thermal energy, allowing atoms to move when they gain sufficient vibrational energy to break the bonds with neighboring atoms. For diffusion to occur, two conditions must be met: there must be vacant sites for atoms to occupy, and the atoms must acquire enough kinetic energy to overcome the energy barriers that keep them bound to their neighbors. At any given temperature, only a fraction of atoms possesses the necessary energy to engage in diffusion, and this fraction increases as the temperature rises. Diffusion in solids, however, is generally a slow process, especially at lower temperatures, where its rate is relatively slow. As temperature increases, diffusion becomes critical in various metallurgical processes such as precipitation, recrystallization, and metal bonding. Karczub and Norton[2], emphasized that diffusion in solids plays a vital role in many processes within

## Diffusing Species into Some Host Metals in Spherical Solids

Akaezue N. Nwagbogwu\*, Ngiangia A. Thompson, and Onyeaju M. Chukwudi

This study investigates the diffusion of various species into host metals in spherical solids. The time-dependent diffusion equation in radial spherical coordinates was transformed into a time-independent form, resulting in a Bessel differential equation of the zeroth kind. The concentration profile within the system was obtained using the Frobenius method. This solution, combined with the fractional Stokes-Einstein model, was used to plot graphs showing the effect of the fractional exponent and temperature on the diffusing species. The results indicate that a rise in temperature leads to early saturation or convergence, followed by divergence, reflecting an increase in the concentration of the diffusing species. Additionally, it was observed that as the fractional exponent increases, the concentration of the diffusing species is enhanced. A model for determining the diffusion coefficient of the host metals is also proposed. The characteristics of the host metals, as shown, significantly affect their diffusion rates. The experimental model is presented alongside the calculated concentration values. The unique approach and findings of this research offer a valuable contribution to diffusion analysis, with potential implications for a wide range of applications involving solid-state materials.

**Keywords:** Diffusion, Host metals, Spherical co-ordinates, Diffusing species.

material science and serves as the foundation for numerous technological applications. The potential of diffusion to drive future technological innovations has attracted the attention of researchers. Bian et al. [3], noted that diffusion continues to be an area of active research due to its broad range of applications. Extensive research has been conducted to understand the relationship between diffusion, self-diffusion, and viscosity, as well as to determine the experimental limits of the Stokes-Einstein equation. While diffusion refers to the movement of atoms or molecules from one site to another, self-diffusion refers to the movement of atoms within a material without any net mass flow. In self-diffusion, the product of the diffusion coefficient and viscosity is constant, validating the Stokes-Einstein equation. However, in cases of regular diffusion, this product is found to be temperature-dependent [4,5]. Surface mobility and diffusion, particularly in glasses, are key factors in understanding the dynamics of glassy materials and their impact on processes such as friction, crystal growth, catalysis, and microfabrication. Metallic glasses, which exhibit distinct structural and bonding properties, offer

intriguing possibilities for exploring surface diffusion. Cao et al. [6] emphasized the importance of understanding the crystallization, nucleation of shear bands, and microfabrication techniques in these materials. The transport properties of Brownian particles in suspensions are also of great interest, especially in complex fluid applications such as food technology and oil recovery. Extensive experimental and theoretical studies have been conducted in this area of research [7]. In crystalline solids, diffusion occurs via atomic hops in a lattice structure. Kapoor and Oyama [8] explain that diffusion in such materials is characterized by a separation of timescales between the elementary jump process of particles between neighboring lattice sites and the macroscopic diffusion process. The elementary atomic jump, which occurs when an atom hops into a neighboring vacancy or interstitial site, lasts for a brief duration, approximately  $10^{-13}$  seconds, corresponding to the reciprocal of the Debye frequency [9]. Understanding diffusion in solids often involves random walk theory. When the electron density in solids is not in equilibrium, electron diffusion occurs. For example, when a bias is applied to a semiconductor or light shines on it, electrons diffuse from regions of high density to regions of low density, forming an electron density gradient and generating a diffusion current [1]. When two miscible liquids are brought into contact, diffusion occurs, and the concentration follows Fick's law. On a mesoscopic scale, between the macroscopic scale governed by Fick's law and the molecular scale where random walk dominates, fluctuations play a significant role. Landau-Lifshitz [9] fluctuating hydrodynamics provides a framework for modeling diffusion in such systems, where fluctuations are taken into account. This theoretical approach shows that diffusion is driven by fluctuations at both molecular and macroscopic scales [10]. The development of diffusion equations, particularly Fick's law, plays a key role in integrated circuit fabrication processes, such as thermal oxidation and doping. Depending on the specific conditions, solutions can be obtained for various boundary conditions like constant source concentration diffusion or moving boundary diffusion. During the processing of metallic materials, they undergo structural transformations, with diffusion playing a critical role in adjusting compositions during solidification [11]. During casting, liquid metal cools to form a solid component. However, conditions may vary, leading to either equilibrium or non-equilibrium solidification. Diffusion is a

time-dependent process, and in solids, diffusion is much slower than in liquids. This concept could also be investigated with selected potential models [12-27]. Equilibrium solidification requires extended periods, which are often impractical. As a result, most solidification processes occur under non-equilibrium conditions, leading to compositional gradients and the formation of metastable phases. Price [28] noted that non-equilibrium cooling can result in phenomena such as segregation and coring, which may need to be corrected through annealing or hot-working. Coring, which is common in alloys with distinct liquidus and solidus temperatures, can be removed through annealing, while segregation is often exploited in zone-refining techniques to produce high-purity metals. Micro-segregation describes compositional differences within a crystal, whereas macro-segregation refers to larger-scale heterogeneities. Santra et al. [29] explain that micro-segregation can be mitigated through annealing, but macro-segregation typically persists through conventional heating and working processes. Motivated by their studies, we intend to determine the temperature and concentration dependent system of diffusion coefficient.

## 2. Formalism

The governing equations that describe theoretically the dynamics of diffusion in a given spherical solid are the diffusion equation in spherical co-ordinates and its complementary equations given as [30],

$$\frac{\partial C}{\partial t} = \frac{D}{r} \left[ \frac{\partial}{\partial r} \left( r^2 \frac{\partial C}{\partial r} \right) + \frac{1}{\sin \theta} \frac{\partial}{\partial \theta} \left( \sin \theta \frac{\partial C}{\partial \theta} \right) + \frac{1}{\sin^2 \theta} \frac{\partial^2 C}{\partial \phi^2} \right] \quad (1)$$

where  $r$  is the radial distance,  $\theta$  is the polar angle and  $\phi$  is the azimuthal angle,  $C$ , is concentration and  $D$  diffusion coefficient.

In considering the radial part of the equation (1) only and simplify, the resulting equation is

$$\frac{\partial C}{\partial t} = D \left( \frac{\partial^2 C}{\partial r^2} + \frac{2}{r} \frac{\partial C}{\partial r} \right) \quad (2)$$

The complementary equations are

$$D = D_0 e^{\beta_1 C} \quad (3)$$

and

$$D = D_o e^{\frac{-E_r}{KT}} \tag{4}$$

where  $\beta_1$  is a constant,  $E_r$ ,  $T$  and  $D_o$  are the activation energy, temperature and pre-exponential factor respectively. A generalized expression for the activation energy is given as [30]

$$E_r = RT^2 \left( \frac{d \ln D}{dT} \right) \tag{5}$$

which incorporate the quantum mechanical tunneling role in the diffusion of the reacting metals. where R is the universal gas constant.

According to Price et al [28], the Fractional Stokes-Einstein relation for diffusion coefficient is given by

$$D = \frac{K_\beta T}{6\pi\mu r^\varepsilon} \tag{6}$$

where,  $K_\beta$  = Boltzmann constant,  $\mu$  is viscosity and  $\varepsilon$  ranges from 0.6-0.9.

The boundary conditions are given as

$$C(r, 0) = 0, C(1, t) = 1, C(2, t) = 2, [9],$$

### 3. Method of Solution

Equation (2) is transformed from time dependent to space dependent equation by using an expression of the form,

$$C = C_{0(r)} e^{-nt} \tag{7}$$

where,  $C_0(r)$  is the characteristic concentration, t is time and n is a constant.

Putting equation (7) into equation (2), gives the resulting Bessel's differential equation of zero kind as

$$C''_{0(r)} + 2r^{-1}C'_{0(r)} + \frac{n}{D}C_{0(r)} = 0 \tag{8}$$

The Frobenius method is given as

$$C_{0(r)} = \sum_{k=0}^{\infty} C_k r^{k+B} \tag{9}$$

Substituting equation (9) into equation (8) and multiply by  $r^{2-k}$ , results into the equation

$$C_k = \frac{n}{D(k+B)(k+B-1)+2(k+B)} C_{k-2} \tag{10}$$

The indicial solution is  $B = 0, -1$

Substituting the values of the indicial solution and simplification for identity results into

$$C = C_o \left( 1 - \frac{n}{6D} r^2 \right) + C_o \left( r^{-1} - \frac{n}{2D} r^1 \right) + C_1 r^1 + C_1 \left( 1 - \frac{n}{6D} r^2 \right) \tag{11}$$

Imposing boundary conditions into equation (11) we have the following resulting equations

$$C_o \left[ \left( 1 - \frac{n}{6D} \right) + \left( 1 - \frac{n}{2D} \right) \right] + C_1 \left[ 1 + \left( 1 - \frac{n}{6D} \right) \right] = 1 \tag{12}$$

$$C_o \left[ \left( 1 - \frac{2n}{3D} \right) + \left( \frac{1}{2} - \frac{n}{D} \right) \right] + C_1 \left[ 2 + \left( 2 - \frac{2n}{3D} \right) \right] = 2 \tag{13}$$

Solve equations (12) and (13) simultaneously to obtain  $C_o$  and  $C_1$  and substitute into equation (11) yields

$$C(r) = \frac{108D^2n + 120Dn^2}{1620D^3 - 1935Dn + 204Dn^2 - 60n^3} \left[ \left( 1 - \frac{n}{6D} r^2 \right) + \left( \frac{1}{r} - \frac{n}{2D} r \right) \right] + \frac{90D^2 + 12Dn}{180D^2 - 15Dn + 6n^2} \left[ r + \left( 1 - \frac{n}{6D} r^2 \right) \right] \tag{14}$$

To determine the diffusion coefficient equation (14) is put into equation (4) and the result is

$$D = D_o e^{\frac{\beta_1}{\left[ \left( 1 - \frac{n}{6D} r^2 \right) + \left( \frac{1}{r} - \frac{n}{2D} r \right) \right] + \frac{90D^2 + 12Dn}{180D^2 - 15Dn + 6n^2} \left[ r + \left( 1 - \frac{n}{6D} r^2 \right) \right]}} \tag{15}$$

Also, from equations (3) and (4), the constant  $\beta_1$  can be stated as

$$\beta_1 = \frac{-E_r}{KTC} \tag{16}$$

4. Results and Discussion

We used the following parameters ( $\varepsilon = 0.6, 0.7, 0.8, 0.9, 1.0$ ;  $r = 1.0, 2.0, 3.0, 4.0, 5.0$ ;  $n = 0.5, 1.0, 1.5, 2.0, 3.0, 4.0, 5.0$ ).  $K_B = 1.380650 \times 10^{-23}$ ;  $T = 5^\circ C, 10^\circ C, 15^\circ C, 20^\circ C, 25^\circ C, 30^\circ C, 40^\circ C, 50^\circ C$ . Figures 1 and 2 show the relationship between concentration and the radius of the diffusing entity for Cu-Cu diffusion, with varying temperature. The data indicate that as the temperature increases from 5°C to 25°C and from 10°C to 50°C, there is convergence at the zero point. It is important to note that this convergence is due to the characteristic property of diffusion, which is influenced by viscosity. However, as the thermal energy increases further, a significant divergence is observed, indicating that at higher temperatures, the concentration of the diffusing species increases substantially. The enhanced thermal energy promotes the internal energy of the diffusing atoms, making diffusion more effective and increasing the diffusion rate. This observation is consistent with Rajput's [1] findings. Figure 3 illustrates the dependence of concentration on the radius of the diffusing entity with varying fractional exponents for Cu-Cu diffusion. When the fractional exponent increases from 0.6 to 1.0, there is early convergence at the zero point, accompanied by an increase in concentration. This suggests that a higher fractional exponent contributes to greater concentration and diffusivity of the diffusing species. This observation aligns with the research of Alope et al. [31]. The plot reveals a saturation at the zero point before diverging exponentially. Figures 4 and 5 depict the concentration dependence on the radius of the diffusing entity for Zn-Cu diffusion, with temperature as the variable. As the temperature rises from 5°C to 25°C and from 10°C to 50°C, early saturation is observed at the zero point, followed by a steady divergence. This behavior signifies an increase in the concentration of the diffusing species at higher temperatures due to increased thermal energy, which enhances the diffusivity. The observations are consistent with Rajput's [1] research. In Figure 6, the dependence of concentration on radius for Zn-Cu diffusion with varying fractional exponents is shown. Early convergence occurs at the zero point, but concentration increases as the fractional exponent rises, likely due to the viscosity of the diffusing species. This behavior agrees with previous findings by Rajput [1]. Figures 7 and 8 illustrate the concentration's dependence on radius for Al-Al diffusion at different temperatures. In both plots, saturation is observed as temperature increases, leading to divergence. However, the divergence in Figure 7

The analysis shows how diffusion behavior varies across different metal systems and under various thermal and fractional exponent conditions. In Figures 8 and 9, for Al-Al diffusion, concentration stabilizes more sharply as temperature rises, a result of heat absorption by diffusing species, aligning with Allen et al. [32]. Figures 10 and 11, for Cu-Ni diffusion, reveal that increased temperatures (5°C to 50°C) promote concentration growth and early saturation at the zero point, with sharp divergence at high thermal energy, consistent with Gao's observations [34].

In Figures 12-15, Cu-Al diffusion demonstrates that concentration rises with temperature and that copper diffuses more readily in aluminum due to stronger Cu-Cu bonds. The effect of viscosity on diffusion is observed with early convergence at the zero point and divergence at higher fractional exponents, aligning with Rajput [1]. For Fe-Fe diffusion, higher temperatures increase diffusion rates, while rising fractional exponents enhance diffusivity and concentration, as confirmed by Hassanabadi and Hosseinpour [36]. Table 1 provides experimental diffusion data, while Table 2 compares calculated coefficients using the Fractional-Stokes-Einstein model. Although slight variations exist, the model accurately predicts diffusion coefficients, reflecting key differences among metals due to viscosities, activation energies, and pre-exponential factors.

This concept can be applied in solid-state physics, as illustrated by the results in Table 3, which were obtained using equation 6.

Table 1 Diffusion Data [1, 48]

Diffusing species	Viscosity $\eta$ (Ns/m <sup>2</sup> )	Host metals	Pre-exponential factors $D_0$ (m <sup>2</sup> /s)	Activation Energy $k$ / mol	Diffusion coefficient $D$ (m <sup>2</sup> /s)
Copper (Cu)	0.44	Cu	$7.8 \times 10^{-5}$	211	$4.2 \times 10^{-19}$
Zinc (Zn)	0.18	Cu	$2.4 \times 10^{-5}$	189	$4.0 \times 10^{-18}$
Aluminum (Al)	0.09	Al	$2.3 \times 10^{-4}$	144	$4.2 \times 10^{-14}$
Copper (Cu)	0.44	Al	$6.5 \times 10^{-5}$	136	$4.1 \times 10^{-14}$
Copper (Cu)	0.44	Nickel (Ni)	$2.7 \times 10^{-5}$	256	$1.3 \times 10^{-22}$

Magnesium (Mg)	0.00936	Al	$1.2 \times 10^{-4}$	131	$1.9 \times 10^{-13}$
Iron (Fe)	0.015	$\alpha$ -Fe BCC	$2.8 \times 10^{-4}$	251	$3.0 \times 10^{-21}$
Iron (Fe)	0.015	$\gamma$ -Fe FCC	$5.0 \times 10^{-5}$	284	$1.1 \times 10^{-17}$

**Table 2: Calculated values of diffusion parameters**

Diffusing species	Viscosities $\eta$ (Ns/m <sup>2</sup> )	Host metals	Pre-exponential factor $D_0$ (m <sup>2</sup> /s)	Activation energy $K$ / mole	constant $\beta$ (mol./kg)	Diffusion coefficient m <sup>2</sup> /s
Copper (Cu)	0.44	Cu	$7.8 \times 10^{-5}$	211	$3.4176747 \times 10^{-18}$	$1.950163 \times 10^{-21}$
Zinc (Zn)	0.18	Cu	$2.4 \times 10^{-5}$	189	$3.652574 \times 10^{-18}$	$4.767065 \times 10^{-21}$
Aluminium (Al)	0.09	Al	$2.3 \times 10^{-4}$	144	$5.610019 \times 10^{-18}$	$9.534132 \times 10^{-21}$
Copper (Cu)	0.44	Al	$6.5 \times 10^{-5}$	136	$1.091165 \times 10^{-17}$	$1.950163 \times 10^{-21}$
Copper (Cu)	0.44	Nickel (Ni)	$2.7 \times 10^{-5}$	256	$4.109416 \times 10^{-18}$	$1.950163 \times 10^{-21}$
Magnesium (Mg)	0.00936	Al	$1.2 \times 10^{-4}$	131	$9.092801 \times 10^{-18}$	$8.910403 \times 10^{-20}$
Iron (Fe)	0.015	$\alpha$ -Fe B.C.C.	$2.8 \times 10^{-4}$	251	$3.5768926 \times 10^{-20}$	$7.400361 \times 10^{-23}$
Iron (Fe)	0.015	$\gamma$ -Fe F.C.C	$5.0 \times 10^{-5}$	284	$2.029269 \times 10^{-19}$	$7.400361 \times 10^{-23}$

**Table 3: Calculated values of concentration parameters**

Diffusing Species	Host metals	Concentration C(Kg/S)
Cu – Cu		1.990
Zn – Cu		3.9960
Al – Al		2.000
Cu – Ni		1.890
Cu – Al		1.988
Mg – Al		2.100
Fe – (α – Fe) BCC		2.000
Fe – (γ – Fe) FCC		1.987

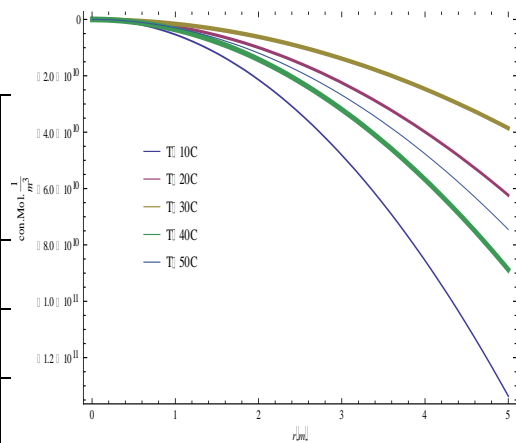


**Figure 2: Dependence of concentration on radius of diffusing entity with temperature varying for Cu-Cu diffusion**

$4.06 \times 10^{-18}$        $1.950163 \times 10^{-21}$   
 $4.09 \times 10^{-18}$        $1.950163 \times 10^{-21}$

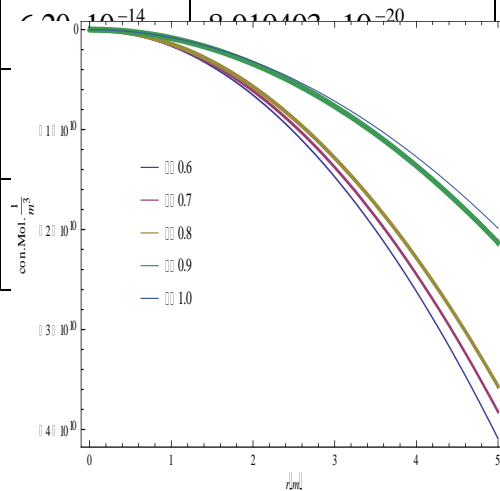


**Figure 3: Dependence of concentration on radius of diffusing entity with fractional exponent varying for Cu-Cu diffusion**

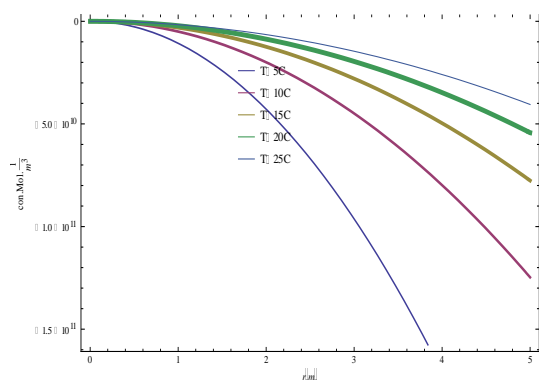


**Figure 1: Dependence of concentration on radius of diffusing entity with temperature varying for Cu-Cu diffusion**

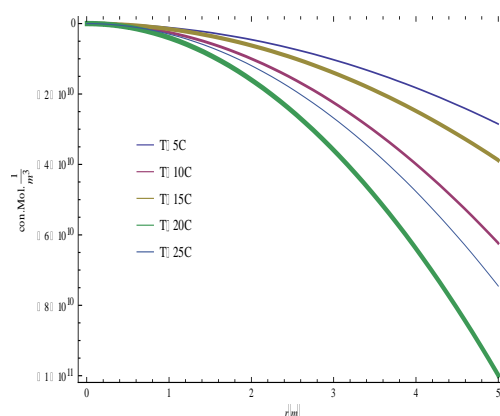


**Figure 4: Dependence of concentration on radius of diffusing entity with temperature varying for Zn-Cu diffusion**

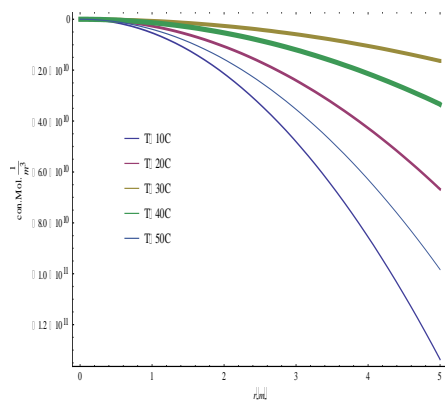


**Figure 5: Dependence of concentration on radius of diffusing entity with temperature varying for Zn-Cu diffusion**

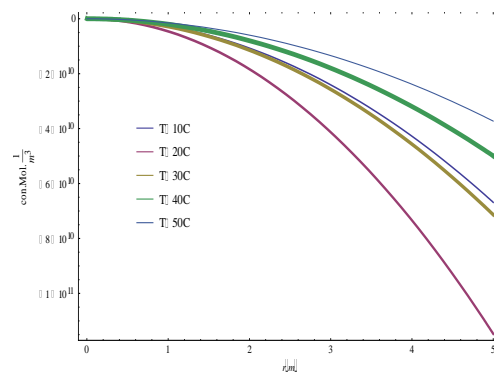


**Figure 8: Dependence of concentration on radius of diffusing entity with temperature varying for Al-Al diffusion**

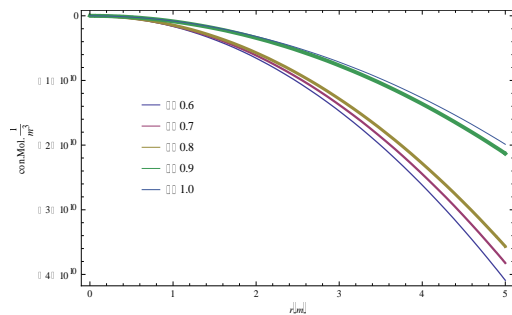


**Figure 6: Dependence of concentration on radius of diffusing entity with fractional exponent varying for Zn-Cu diffusion**

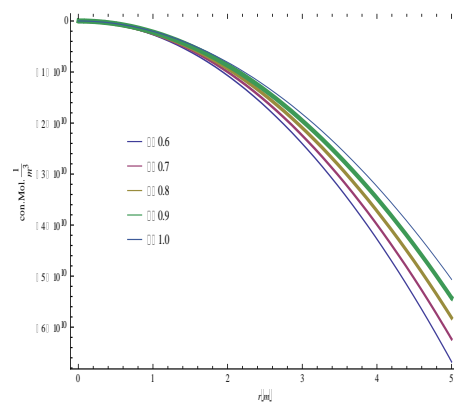


**Figure 9: Dependence of concentration on radius of diffusing entity with fractional exponent varying for Al-Al diffusion**

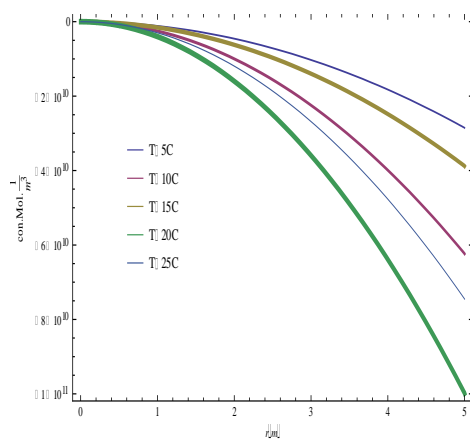


**Figure 7: Dependence of concentration on radius of diffusing entity with temperature varying for Al-Al diffusion**

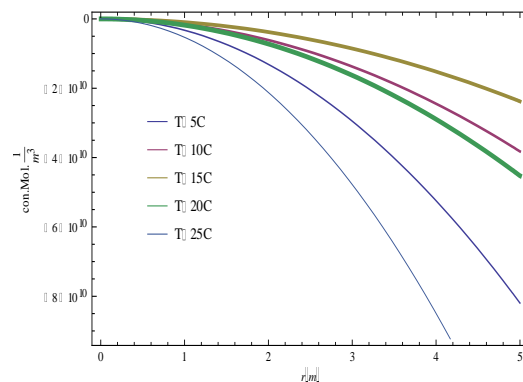


**Figure 10: Dependence of concentration on radius of diffusing entity with temperature varying for Cu-Ni diffusion**

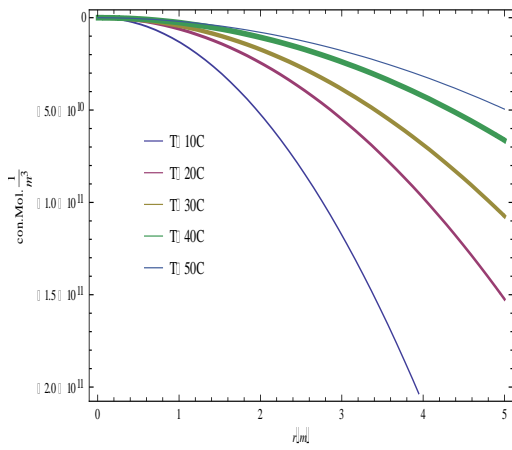


**Figure 11: Dependence of concentration on radius of diffusing entity with temperature varying for Cu-Ni diffusion**

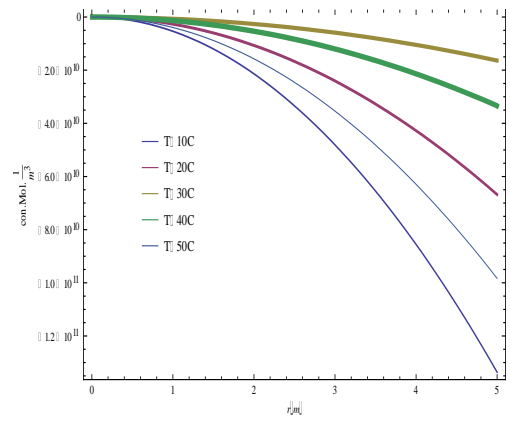


**Figure 14: Dependence of concentration on radius of diffusing entity with temperature varying for Cu-Al diffusion**

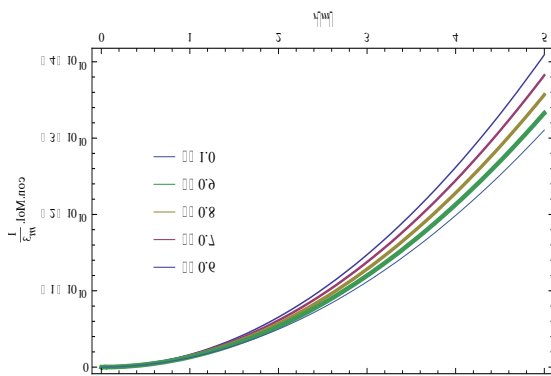


**Figure 12: Dependence of concentration on radius of diffusing entity with fractional exponent varying for Cu-Ni diffusion**

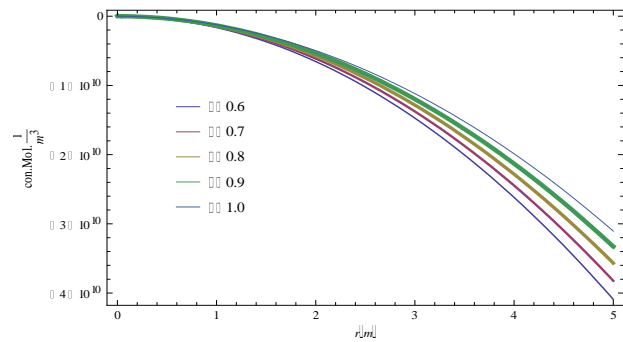


**Figure 15: Dependence of concentration on radius of diffusing entity with fractional exponent varying for Cu-Al diffusion**

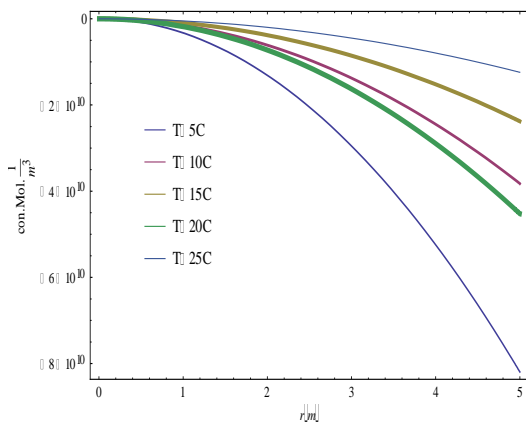


**Figure 13: Dependence of concentration on radius of diffusing entity with temperature varying for Cu-Al diffusion**

### 5. Conclusion

This study provides an analytical approach to species diffusion in spherical solids, validating the fractional Stokes-Einstein model as a more precise tool for estimating diffusion coefficients in metals. Unlike prior studies, it explores fractional exponents extending to Einstein's upper limit of 1, expanding the scope for diffusion analysis. Additionally, using spherical rather than rectangular coordinates allows for a more accurate representation of diffusion in these materials. The findings highlight the influence of atomic size on diffusion rates, offering insights crucial for optimizing material properties in applications such as alloy fabrication, metallurgy, and semiconductor device performance.

### Conflict of interest

The authors declare no conflict of interest.

### Acknowledgements

Akaezue Nelson Nwagbogwu sincerely acknowledges the support of the Theoretical Physics group university of Port Harcourt.



## References

- [1] Rajput, R. K. (2013). *Material science and engineering* (Third Edition). S.K. Kataria Books and Sons, New Delhi.
- [2] Karczub, D. G., & Norton, M. P. (2003). *Fundamentals of noise and vibration analysis for engineers*. <https://doi.org/10.3397/1.2721371>
- [3] Bian, X., Kim, C., & Karniadakis, G. E. (2016). 111 years of Brownian motion. *Soft Matter*, 12(30), 6331–6346. <https://doi.org/10.1039/c6sm01153e>
- [4] Hung, V. V., Tich, H. V., & Masuda-Jindo, K. (2000). Study of self-diffusion in metals by statistical moment method. *Journal of the Physical Society of Japan*, 69(8), 2691–2699. <https://doi.org/10.115/2018/5462659>
- [5] Vázquez, J. L. (2006). *The porous medium equation: Mathematical theory*. <https://doi.org/10.1093/acprof:oso/9780198569039.001.0001>
- [6] Cao, C., & Lu, R. Y. M. (2015). High surface mobility and fast surface-enhanced crystallization of metallic glass. *American Institute of Physics*. <https://doi.org/10.1063/1.4933036>
- [7] Matthias, K., & Markus, R. (2009). Diffusion of a sphere in a dilute solution of polymer coils. <https://doi.org/10.1063/1.3216108>
- [8] Kapoor, R., & Oyama, S. T. (2011). Measurement of solid diffusion coefficient by a temperature-programmed method. *Journal of Materials Research*, 12(2). <https://doi.org/10.1557/JMR1997.0068>
- [9] Helmut, M. (2007). *Diffusion in solids*. Springer Series in Solid-State Science. <https://doi.org/10.1007/978-3-540-71488-0>
- [10] Okamoto, H. (2013). Thermodynamic reassessment of the binary Cu-Sn, Cu-P, and Sn-P, and ternary Cu-Sn-P system. *Journal of Phase Equilibria and Diffusion*, 33, 25. <https://doi.org/10.1016/11998-012-385938900005->
- [11] Mandelbrot, B., & Hyndson, R. (2004). *The misbehavior of market: A fractional view of risk, ruin, and reward*. Basic Books. [dichgiacamch.files.wordpress.com](https://dichgiacamch.files.wordpress.com)
- [12] Inyang, E., & Obisung, E. (2022). The study of electronic states of NI and Scl molecules with screened Kratzer Potential. *East European Journal of Physics*, (3), 32-38. <https://doi.org/10.26565/2312-4334-2022-3-04>
- [13] William, E. S., Inyang, E. P., Akpan, I. O., Obu, J. A., Nwachukwu, A. N., & Inyang, E. P. (2022). Ro-vibrational energies and expectation values of selected diatomic molecules via Varshni plus modified Kratzer potential model. *Indian Journal of Physics*, 96(12), 3461-3476. <https://doi.org/10.1007/s12648-022-02308-0>
- [14] Inyang, E. P., & Ita, B. I. (2021). Relativistic treatment of Quantum mechanical Gravitational-Harmonic Oscillator potential. *European Journal of Applied Physics*, 3(3), 42-47. <http://dx.doi.org/10.24018/ejphysics.2021.3.3.83>
- [15] Inyang, E. P., Obisung, E. O., Amajama, J., Basse, D. E., William, E. S., & Okon, I. B. (2022). The effect of topological defect on the mass spectra of heavy and heavy-light quarkonia. *Eurasian Physical Technical Journal*, 19(4), 78-87. <https://doi.org/10.31489/2022No4/78-87>
- [16] Ibekwe, E. E., Inyang, E. P., Emah, J. B., Akpan, J. B., & Yawo, O. J. (2022). Mass spectra and thermal properties of the deformed Schrödinger equation for pseudoharmonic potential. *Sri Lankan Journal of Physics*, 23(2), 63–76. <http://doi.org/10.4038/sljp.v23i2.8119>
- [17] Inyang, E. P., Okon, I. B., Faithpraise, F. O., William, E. S., Okoi, P. O., & Ibanga, E. A. (2023). Quantum mechanical treatment of Shannon entropy measure and energy spectra of selected diatomic molecules with the modified Kratzer plus generalized inverse quadratic Yukawa potential model. *Journal of Theoretical and Applied Physics*, 17(4). <https://dx.doi.org/10.57647/j.jtap.2023.1704.40>
- [18] Inyang, E. P., Faithpraise, F. O., Amajama, J., William, E. S., Obisung, E. O., & Ntibi, J. E. (2023). Theoretical investigation of meson spectrum using exact quantization rule technique. *East European Journal of Physics*, 1, 53-62. <https://doi.org/10.26565/2312-4334-2023-1-05>
- [19] Inyang, E. P., Omugbe, E., Abu-shady, M., & William, E. S. (2023). Investigation of quantum information theory with the screened modified Kratzer and a class of Yukawa potential model. *The European Physical Journal Plus*, 138(11), 969. DOI : 10.1140/epjp/s13360-023-04617-7

- [20] Abu-Shady, M., & Inyang, E. P. (2023). The Fractional Schrödinger Equation with the Generalized Woods-Saxon Potential. *East Eur. J. Phys.*, 2023(arXiv: 2302.03060), 63-68.
- [21] Inyang, E. P., William, E. S., Omugbe, E., & Ayedun, F. (2023). The study of H<sub>2</sub> and N<sub>2</sub> diatomic molecules in arbitrary dimensions with the collective potential model. *Bulgarian Journal of Physics*, 50(3), 265–279. <https://doi.org/10.55318/bgjp.2023.50.3.265>
- [22] Ibekwe, E. E., Emah, J. B., Inyang, E. P., & Akpan, A. O. (2022). MASS Spectrum of Heavy Quarkonium for Combined Potentials (Modified Kratzer Plus Screened Coulomb Potential). *Iranian Journal of Science and Technology, Transactions A: Science*, 46(6), 1741-1748. <https://doi.org/10.1007/s40995-022-01377-4>
- [23] Patrick, I. E., Joseph, N., Akpan, I. E., Funmilayo, A., Peter, I. E., & Sunday, W. E. (2023, January). Thermal properties, mass spectra and root mean square radii of heavy quarkonium system with class of inversely quadratic Yukawa potential. In *AIP Conference Proceedings* (Vol. 2679, No. 1). AIP Publishing. <https://doi.org/10.1063/5.0112829>
- [24] Obu, J. A., William, E. S., Akpan, I. O., Thompson, E. A., & Inyang, E. P. (2020). Analytical Investigation of the Single-particle energy spectrum in Magic Nuclei of 56Ni and 116Sn. *Eur. J. Appl. Phys.*, 2(1). <http://dx.doi.org/10.24018/ejphysics.2020.2.6.28>.
- [25] Thompson, E. A., Inyang, E. P., & William, E. S. (2021). Analytical determination of the non-relativistic quantum mechanical properties of near doubly magic nuclei. *Physical Sciences and Technology*, 8(3-4), 10-21. <https://doi.org/10.26577/phst.2021.v8.i2.02>
- [26] Faithpraise, F. O., & Inyang, E. P. (2023). Bound state and ro-vibrational energies eigenvalues of selected diatomic molecules with a class of inversely quadratic Yukawa plus Hulthén potential model. *East European Journal of Physics*, (3), 158-166. DOI:10.26565/2312-4334-2023-3-12
- [27] William, E. S., Inyang, E. P., & Thompson, E. A. (2020). Arbitrary l-solutions of the Schrödinger equation interacting with Hulthén-Hellmann potential model. *Revista mexicana de física*, 66(6), 730-741. 10.31349/RevMexFis.66.730.
- [28] Price, H. C., Mattsson, J., & Murray, B. J. (2016). Sucrose diffusion in aqueous solution. *Journal of Physical Chemistry*, 18(28), 19207-19216. doi:10.1039/c6cp03238A.
- [29] Santra, S., Islam, R., Ravi, V., Vuorinen, T., Laurila, A., & Paul, A. (2014). Phase evolutions in AuCu/Sn system by solid state reactive diffusion. *Journal of Electronic Materials*. <https://doi.org/10.1007/s11664-014-3241-z>
- [30] Akaezue, N.N., Ngiangia, A.T & Onyeaju, M.C. (2024). Thermal properties of diffusing species into some host metals. *Communication in physical sciences*, 11(4):809-818
- [31] Aloke, P. (2014). *Thermodynamics, diffusion and the Kirkendall effect in solids*. Springer. *Journal of Applied Physics*, 91. ISBN 331907461X, 9783319074610
- [32] Allen, M. P., & Tildesley, D. J. (2017). *Computer simulation of liquids*. Oxford Scholarship Online. <https://doi.org/10.1093/030/9780198803195.001.0001>
- [33] B Gusak, A. M., Lyashenko, Y., & Kornienko, V. S. (2010). Diffusion-controlled solid-state reactions: In alloys, thin films, and nano-systems. <https://doi.org/10.1002/97834631025>
- [34] Gao, X. (2022). The mathematics of the ensemble theory. *Results in Physics*. <https://doi.org/10.1016/j.rinp.2022.105230>
- [35] Leshner, C. E. (2015). Thermodynamic and transport properties of silicate melts and magma. *The Encyclopedia of Volcanoes*. <https://doi.org/10.1016/11998-012-385938900005-5>
- [36] Hassanabadi, H., & Hosseinpour, M. (2016). Thermodynamic properties of neutral particle in the presence of topological defects in magnetic cosmic string background. *European Physical Journal*, 76, 553. Doi :10.1140/epjp/s13360-020-0046-9.
- [37] Bartsch, A., Zollmer, V., et al. (2011). Diffusion and viscous flow in bulk glass-forming alloys. *Journal of Alloys and Compounds*. <https://doi.org/10.1016/j.allcom.2010.11123>
- [38] Belkin, A. (2015). Self-assembled wiggling nanostructures and the principles of maximum entropy production. *Scientific Reports*, 5(1), 8323. <https://doi.org/10.1038/srep08323>

[39] Brogioli, D., & Vailati, A. (2001). Diffusive mass transfer by nonequilibrium fluctuations: Fick's law revisited. *Physical Review E*, 63(1-4), 012105.

<https://doi.org/10.1103/PhysRevE.63.012105>

[40] Chang, Y. A., & Neumann, J. P. (1982). The elastic constants of the intermetallic compound from 77k to 900k. [https://doi.org/10.1016/0022-3696\(77\)90234](https://doi.org/10.1016/0022-3696(77)90234)

[41] Chaudhuri, G., & Gupta, S. (2007). Specific heat and bimodality in canonical and grand canonical versions of the thermodynamic model. *Physics Review C*, 76(1), 014619. <https://doi.org/10.1103/PhysRevC.76a014619>

[42] Chen, J. (2020). Stochastic absorption of diluted solute molecules at interfaces. *ChemRxiv*. <https://doi.org/10.26434/chemrxiv-2021-g4zp8-v3>

[43] Cserháti, A., Paul, A., Kodentsov, A. A., Aloke, P., & van Dal, M. (2003). On the spatial stability and bifurcation of the Kirkendall plane during solid-state interdiffusion. <https://doi.org/10.1080/10408430802462958>

[44] Divya, U., Ramamurty, P., & Paul, A. (2012). *Philosophical Magazine*, 92, 2187. <https://doi.org/10.1038/srep08323>

[45] Gorban, A. N., Sargsyan, H. P., & Wahab, H. A. (2011). Quasichemical models of multicomponent nonlinear diffusion. *Mathematical Modelling of Natural Phenomena*, 6(5), 184-262. <https://doi.org/10.1051/mmnp/20116509>

[46] Guo, W., Yuan, Y., Sun, Z., Cai, Z., & Qiao, Z. (2009). The impact of nonlinear losses in the silicon micro-ring cavities on CW pumping correlated photon pair generation. *Journal of Optic Express*, 22, 2620-2631. doi: 10.1364/OE22002620

[47] Morozov, A. N., & Skripkin, A. V. (2011). Spherical particle Brownian motion in viscous medium as non-markovian random process. *Physics Letters A*, 375(46), 4113-4115. doi:10.1016/j.physleta.2011.10.001

[48] Hilderbrand, J.H. and Lamoreaux, R. H. (1977). Fluidity and Liquid Structure. *Journal of physical chemistry* vol.:77 (11) .:https://doi.org/10.1073/pnas.73.4.988